

20

Currents on Linear Antennas

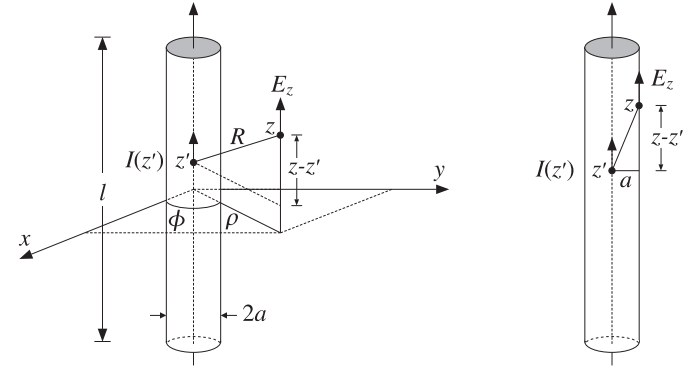


Fig. 20.1.1 Thin-wire model of cylindrical antenna.

20.1 Hallén and Pocklington Integral Equations

In Sec. 13.4, we determined the electromagnetic fields generated by a given current distribution on a thin linear antenna, but did not discuss the mechanism by which the current distribution is set up and maintained. In Chap. 15, we assumed that the currents were sinusoidal, but this was only an approximation. Here, we discuss the integral equations that determine the exact form of the currents.

An antenna, whether transmitting or receiving, is always driven by an external source field. In transmitting mode, the antenna is driven by a generator voltage applied to its input terminals, and in receiving mode, by an incident electric field (typically, a uniform plane wave if it is arriving from far distances.) In either case, we will refer to this external source field as the “incident” field E_{in} .

The incident field E_{in} induces a current on the antenna. In turn, the current generates its own field E , which is radiated away. The total electric field is the sum $E_{tot} = E + E_{in}$. Assuming a perfectly conducting antenna, the *boundary conditions* are that the tangential components of the total electric field vanish on the antenna surface. These boundary conditions are enough to determine the current distribution induced on the antenna.

Fig. 20.1.1 depicts a z -directed thin cylindrical antenna of length l and radius a , with a current distribution $I(z)$ along its length. We will concentrate only on the z -component E_z of the electric field generated by the current and use cylindrical coordinates.

For a perfectly conducting antenna, the current is essentially a surface current at radial distance $\rho = a$ and surface density $J_s(z) = \hat{z}I(z)/2\pi a$. The corresponding volume current density will be as in Eq. (13.4.2):

$$\mathbf{J}(\mathbf{r}) = J_s(z)\delta(\rho - a) = \hat{z}I(z)\delta(\rho - a)\frac{1}{2\pi a}$$

Following the procedure of Sec. 13.4, we obtain the z -component of the vector potential:

$$\begin{aligned} A_z(z, \rho, \phi) &= \frac{\mu}{4\pi} \int_{V'} \frac{I(z')\delta(\rho' - a)e^{-jkR}}{2\pi aR} \rho' d\rho' d\phi' dz' \\ &= \frac{\mu}{4\pi} \int_{-l/2}^{l/2} \int_0^{2\pi} \frac{I(z')e^{-jkR}}{2\pi R} d\phi' dz' \end{aligned}$$

where $R = |\mathbf{r} - \mathbf{r}'| = \sqrt{(z - z')^2 + |\boldsymbol{\rho} - \boldsymbol{\rho}'|^2}$. Because $\rho' = a$, we have:

$$|\boldsymbol{\rho} - \boldsymbol{\rho}'|^2 = \rho^2 + a^2 - 2\rho \cdot \boldsymbol{\rho}' = \rho^2 + a^2 - 2\rho a \cos(\phi' - \phi)$$

Because ϕ' appears only through the difference $\phi' - \phi$, we may change the variable of integration from ϕ' to $\phi' - \phi$. This implies that A_z will be cylindrically symmetric, that is, independent of ϕ . It follows that:

$$A_z(z, \rho) = \frac{\mu}{4\pi} \int_{-l/2}^{l/2} I(z')K(z - z', \rho) dz' \quad (20.1.1)$$

where we defined the kernel:

$$K(z - z', \rho) = \frac{1}{2\pi} \int_0^{2\pi} \frac{e^{-jkR}}{R} d\phi' \quad (20.1.2)$$

with $R = \sqrt{(z - z')^2 + \rho^2 + a^2 - 2\rho a \cos\phi'}$. In the limit of a thin antenna, $a \rightarrow 0$, Eq. (20.1.1) reduces to:

$$A_z(z, \rho) = \frac{\mu}{4\pi} \int_{-l/2}^{l/2} I(z')G(z - z', \rho) dz' \quad (20.1.3)$$

where $G(z - z', \rho)$ is the *reduced thin-wire kernel*:

$$G(z - z', \rho) = \frac{e^{-jkR}}{R}, \quad R = \sqrt{(z - z')^2 + \rho^2} \quad (20.1.4)$$

Eq. (20.1.3) is the same as (13.4.3) because the limit $a = 0$ is equivalent to assuming that the current density is a line current $\mathbf{J}(\mathbf{r}) = \hat{z}I(z)\delta(x)\delta(y)$, as given by Eq. (13.4.1). In practice the thin-wire approximation is adequate.

Given the vector potential A_z , the z -component of the electric field generated by the current is obtained from Eq. (13.4.6):

$$j\omega\mu\epsilon E_z = (\partial_z^2 + k^2)A_z \quad (20.1.5)$$

Even though we took the limit as $a \rightarrow 0$, it is still meaningful to consider the boundary conditions at the cylindrical surface of the antenna, as shown on the right of Fig. 20.1.1. Evaluating Eqs. (20.1.3) and (20.1.4) at $\rho = a$, we obtain:

$$A_z(z) = \frac{\mu}{4\pi} \int_{-l/2}^{l/2} I(z') G(z - z') dz' \quad (20.1.6)$$

where we denoted $A_z(z) = A_z(z, a)$ and $G(z - z') = G(z - z', a)$:

$$G(z - z') = \frac{e^{-jkR}}{R}, \quad R = \sqrt{(z - z')^2 + a^2} \quad (20.1.7)$$

The boundary condition on the surface is that the z -component of the total electric field vanish, that is, at $\rho = a$:

$$E_{z,\text{tot}}(z, \rho) = E_z(z, \rho) + E_{z,\text{in}}(z, \rho) = 0$$

Thus, with $E_z(z) = E_z(z, a)$ and $E_{\text{in}}(z) = E_{z,\text{in}}(z, a)$, we have $E_z(z) = -E_{\text{in}}(z)$, and Eq. (20.1.5) can be expressed in terms of the z -component of the incident field:

$$(\partial_z^2 + k^2) A_z(z) = -j\omega\mu\epsilon E_{\text{in}}(z) \quad (20.1.8)$$

To summarize, given an incident field $E_{\text{in}}(z)$ that is known along the length of the antenna, Eq. (20.1.8) may be solved for $A_z(z)$ and then the integral equation (20.1.6) can be solved for the current $I(z)$.

Depending on how this procedure is carried out, one obtains either the Hallén or the Pocklington equations. Solving Eq. (20.1.8) by formally inverting the differential operator $(\partial_z^2 + k^2)$ and combining with (20.1.6), we obtain *Hallén's integral equation*:

$$\frac{\mu}{4\pi} \int_{-l/2}^{l/2} I(z') G(z - z') dz' = -j\omega\mu\epsilon (\partial_z^2 + k^2)^{-1} E_{\text{in}}(z) \quad (20.1.9)$$

Alternatively, applying the differential operator $(\partial_z^2 + k^2)$ directly to Eq. (20.1.6) and combining with (20.1.8), we obtain *Pocklington's integral equation*:

$$\frac{\mu}{4\pi} \int_{-l/2}^{l/2} I(z') (\partial_z^2 + k^2) G(z - z') dz' = -j\omega\mu\epsilon E_{\text{in}}(z) \quad (20.1.10)$$

The two integral equations must be solved subject to the constraint that the current $I(z)$ vanish at the antenna ends, that is, $I(l/2) = I(-l/2) = 0$.

Hallén's equation involves a simpler and numerically better-behaved kernel than Pocklington's. The inverse differential operator in the right-hand side of Eq. (20.1.9) can be rewritten as an integral convolutional operator acting on E_{in} . We discuss this in detail in Sec. 20.3.

20.2 Delta-Gap and Plane-Wave Sources

Although the external source field $E_{\text{in}}(z)$ can be specified arbitrarily, there are two special cases of practical importance. One is the so-called delta-gap model, which imitates the way a transmitting antenna is fed by a transmission line. The other is a uniform plane wave incident at an angle on a receiving antenna connected to a load impedance. Fig. 20.2.1 depicts these cases.

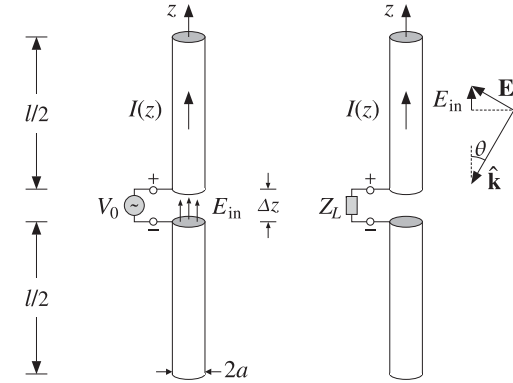


Fig. 20.2.1 External sources acting on a linear antenna.

The left figure shows the *delta-gap* model of a generator voltage applied between the upper and lower halves of the antenna across a short gap of length Δz . The applied voltage V_0 can be thought of as arising from an electric field—the “incident” field in this case—which exists only within the gap, such that

$$V_0 = \int_{-\Delta z/2}^{\Delta z/2} E_{\text{in}}(z) dz \quad (20.2.1)$$

A simplified case arises when we take the limit $\Delta z \rightarrow 0$. Then, approximately, $V_0 = E_{\text{in}}\Delta z$, or $E_{\text{in}} = V_0/\Delta z$. In order to maintain a finite value of V_0 in the left-hand side of Eq. (20.2.1), E_{in} must become commensurately large. This means that in this limit,

$$E_{\text{in}}(z) = V_0\delta(z) \quad (\text{delta-gap model of incident field}) \quad (20.2.2)$$

King [3] has discussed the case of a finite Δz . Fig. 20.2.1 shows on the right a receiving antenna with a uniform plane wave incident at a polar angle θ and such that the propagation vector $\hat{\mathbf{k}}$ is co-planar with the antenna axis.

The electric field vector is perpendicular to $\hat{\mathbf{k}}$ and has a space dependence $E_0 e^{-j\mathbf{k}\cdot\mathbf{r}}$. For a thin antenna, we may evaluate the field along the z -axis, that is, we set $x = y = 0$ so that $e^{-j\mathbf{k}\cdot\mathbf{r}} = e^{-jk_z z} = e^{jk_z \cos\theta}$ because $k_z = -k \cos\theta$. Then, the z -component of the incident field will be:

$$E_{\text{in}}(z) = E_0 \sin\theta e^{jk_z \cos\theta} \quad (\text{incident uniform plane wave}) \quad (20.2.3)$$

If the wave is incident from broadside ($\theta = \pi/2$), then $E_{\text{in}}(z) = E_0$, that is, a constant along the antenna length. And, if $\theta = 0$ or π , then $E_{\text{in}}(z) = 0$.

20.3 Solving Hallén's Equation

Instead of working with the vector potential $A_z(z)$ it proves convenient to work with a scaled version of it that has units of volts and is defined as:

$$V(z) = 2jcA_z(z) \quad (20.3.1)$$

where c is the speed of light. We note that $V(z)$ is not the scalar potential $\varphi(z)$ along the antenna length. From the Lorenz condition, Eq. (13.4.5), we have $\partial_z A_z = -j\omega\mu\epsilon\varphi(z)$. Multiplying by $2jc$ and noting that $c\omega\epsilon\mu = \omega/c = k$, we find:

$$\partial_z V(z) = 2k\varphi(z) \quad (20.3.2)$$

Multiplying both sides of Eq. (20.1.8) by $2jc$, we can rewrite it as:

$$\boxed{(\partial_z^2 + k^2)V(z) = 2kE_{in}(z)} \quad (20.3.3)$$

Similarly, Eq. (20.1.6) becomes:

$$\boxed{\int_{-h}^h Z(z-z')I(z')dz' = V(z)} \quad (20.3.4)$$

where for later convenience, we introduced the *half-length* of the antenna $h = l/2$ and defined the “impedance” kernel:

$$\boxed{Z(z-z') = \frac{j\eta}{2\pi}G(z-z') = \frac{j\eta}{2\pi} \frac{e^{-jkR}}{R}}, \quad R = \sqrt{(z-z')^2 + a^2} \quad (20.3.5)$$

where $\eta = \sqrt{\mu/\epsilon}$. Eqs. (20.3.3)–(20.3.5) represent our rescaled version of Hallén's equations. Formally, we can write $V(z) = 2k(\partial_z^2 + k^2)^{-1}E_{in}(z)$, but we prefer to express $V(z)$ as an integral operator acting on $E_{in}(z)$.

A particular solution of (20.3.3) is obtained with the help of the Green's function $F(z)$ for this differential equation:

$$\boxed{(\partial_z^2 + k^2)F(z) = 2k\delta(z)} \quad (20.3.6)$$

The general solution of Eq. (20.3.3) is obtained by adding the most general solution of the homogeneous equation, $(\partial_z^2 + k^2)V(z) = 0$, to the Green's function solution:

$$V(z) = C_1 e^{jkz} + C_2 e^{-jkz} + \int_{-h}^h F(z-z')E_{in}(z')dz' \quad (20.3.7)$$

With a re-definition of the constants C_1, C_2 , we can also write:

$$V(z) = C_1 \cos kz + C_2 \sin kz + \int_{-h}^h F(z-z')E_{in}(z')dz' \quad (20.3.8)$$

In fact, $F(z)$ itself is defined up to an arbitrary solution of the homogeneous equation. If $F(z)$ satisfies Eq. (20.3.6), so does $F_1(z) = F(z) + C_1 e^{jkz} + C_2 e^{-jkz}$, with arbitrary

constants C_1, C_2 . Some possible choices for $F(z)$ are as follows. They differ from each other by a homogeneous term:

$$\boxed{\begin{aligned} F_1(z) &= je^{-jk|z|} = F_2(z) + j \cos kz \\ F_2(z) &= \sin k|z| = F_3(z) - \sin kz \\ F_3(z) &= 2 \sin(kz)u(z) = F_4(z) + 2 \sin kz \\ F_4(z) &= -2 \sin(kz)u(-z) \end{aligned}} \quad (20.3.9)$$

where $u(z)$ is the unit-step function. All satisfy Eq. (20.3.6) as well as the required discontinuity conditions on their first derivative, that is,

$$F'(0+) - F'(0-) = 2k \quad (20.3.10)$$

This discontinuity condition is obtained by integrating Eq. (20.3.6) over the small interval $-\epsilon \leq z \leq \epsilon$ and then taking the limit $\epsilon \rightarrow 0$ and assuming that $F(z)$ itself is continuous at $z = 0$. Depending on the choice of $F(z)$, the corresponding solution $V(z)$ can be written in the equivalent forms (each with different C_1, C_2):

$$\begin{aligned} V(z) &= C_1 e^{jkz} + C_2 e^{-jkz} + \int_{-h}^h je^{-jk|z-z'|} E_{in}(z') dz' \\ V(z) &= C_1 e^{jkz} + C_2 e^{-jkz} + \int_{-h}^h \sin(k|z-z'|) E_{in}(z') dz' \\ V(z) &= C_1 e^{jkz} + C_2 e^{-jkz} + 2 \int_{-h}^z \sin(k(z-z')) E_{in}(z') dz' \\ V(z) &= C_1 e^{jkz} + C_2 e^{-jkz} - 2 \int_z^h \sin(k(z-z')) E_{in}(z') dz' \end{aligned} \quad (20.3.11)$$

We will use mostly the first and second choices for $F(z)$, that is, $F(z) = je^{-jk|z|}$ and $F(z) = \sin k|z|$. Combining the solution for $V(z)$ with Eq. (20.3.4), we obtain the equivalent form of Hallén's integral equation:

$$\boxed{\int_{-h}^h Z(z-z')I(z')dz' = C_1 e^{jkz} + C_2 e^{-jkz} + \int_{-h}^h F(z-z')E_{in}(z')dz'} \quad (20.3.12)$$

or, alternatively,

$$\int_{-h}^h Z(z-z')I(z')dz' = C_1 \cos kz + C_2 \sin kz + \int_{-h}^h F(z-z')E_{in}(z')dz'$$

The constants C_1, C_2 are determined from the end conditions $I(h) = I(-h) = 0$. Next, we consider the particular forms of Eq. (20.3.12) in the delta-gap and plane-wave cases. In the delta-gap case, we have $E_{in}(z) = V_0\delta(z)$ and the integral on the right-hand side can be done trivially, giving:

$$\int_{-h}^h F(z-z')E_{in}(z')dz' = \int_{-h}^h F(z-z')V_0\delta(z')dz' = V_0F(z)$$

Thus, we have the integral equation:

$$\int_{-h}^h Z(z - z')I(z') dz' = C_1 \cos kz + C_2 \sin kz + V_0 F(z)$$

We expect the current $I(z)$ to be an even function of z (because $E_{in}(z)$ is), and thus we may drop the C_2 term. Using $F(z) = \sin k|z|$ as our Green's function choice, we obtain *Hallén's equation for the delta-gap case*:

$$\int_{-h}^h Z(z - z')I(z') dz' = V(z) = C_1 \cos kz + V_0 \sin k|z| \tag{20.3.13}$$

This equation forms the basis for determining the current on a center-driven linear antenna. We will consider several approximate solutions of it as well as numerical solutions based on moment methods.

We can verify that $V(z)$ correctly gives the potential difference between the upper and lower halves of the antenna. Differentiating $V(z)$ about $z = 0$ and using Eq. (20.3.2), we have:

$$V'(0+) - V'(0-) = 2kV_0 = 2k(\varphi(0+) - \varphi(0-)) \Rightarrow \varphi(0+) - \varphi(0-) = V_0$$

As a second example, consider the case of an antenna receiving a uniform plane wave with incident field as in Eq. (20.2.3). Using $F(z) = je^{-jk|z|}$ as the Green's function, the convolution integral of $F(z)$ and $E_{in}(z)$ can be done easily giving:

$$\int_{-h}^h je^{-jk|z-z'|} E_0 \sin \theta e^{jkz' \cos \theta} dz' = \frac{2E_0}{k \sin \theta} e^{jkz \cos \theta} + (\text{homogeneous terms})$$

where the last terms are solutions of the homogeneous equation, and thus, can be absorbed into the other homogeneous terms of $V(z)$. Because the current is not expected to be symmetric in z , we must keep both homogeneous terms, resulting in *Hallén's equation for a receiving antenna*:

$$\int_{-h}^h Z(z - z')I(z') dz' = V(z) = C_1 e^{jkz} + C_2 e^{-jkz} + \frac{2E_0}{k \sin \theta} e^{jkz \cos \theta} \tag{20.3.14}$$

20.4 Sinusoidal Current Approximation

Here, we look at simplified solutions of Eq. (20.3.13), which justify the common sinusoidal assumption for the current.

Inspecting the kernel $Z(z - z')$ or $G(z - z') = e^{-jkR}/R$ of the integral equation (20.3.13), we note that as the integration variable z' sweeps past z , the denominator becomes very large, because $R = a$ at $z' = z$. Therefore, the integral is dominated by the value of the integrand near $z' = z$. We can write approximately,

$$\int_{-h}^h Z(z - z')I(z') dz' \approx \bar{Z}(z)I(z) \approx \bar{Z}I(z) \tag{20.4.1}$$

where $\bar{Z}(z)$ is a sort of an average value of $Z(z - z')$ in the neighborhood of $z' = z$. This quantity varies slowly with z and we may approximate it with a constant, say \bar{Z} . Then, Hallén's equation (20.3.13) becomes approximately:

$$\bar{Z}I(z) = V(z) = C_1 \cos kz + V_0 \sin k|z|$$

This shows that $I(z)$ is approximately sinusoidal. The constant C_1 is fixed by the end-condition $I(h) = 0$, which gives:

$$C_1 \cos kh + V_0 \sin kh = 0 \Rightarrow C_1 = -V_0 \frac{\sin kh}{\cos kh}$$

so that $I(z)$ becomes:

$$\bar{Z}I(z) = -V_0 \frac{1}{\cos kh} [\sin kh \cos kz - \cos kh \sin k|z|] = -V_0 \frac{1}{\cos kh} \sin(k(h - |z|))$$

Solving for $I(z)$, we obtain the common standing-wave expression for the current:

$$I(z) = I(0) \frac{\sin(k(h - |z|))}{\sin kh}, \quad I(0) = -\frac{V_0 \sin kh}{\bar{Z} \cos kh} \tag{20.4.2}$$

where $I(0)$ is the input current at $z = 0$. The crude approximation of Eq. (20.4.1) can be refined further using King's three-term approximation discussed in Sec. 20.6. From Eq. (20.4.2), the antenna input impedance is seen to be:

$$Z_A = \frac{V_0}{I(0)} = -\bar{Z} \cot kh \tag{20.4.3}$$

20.5 Reflecting and Center-Loaded Receiving Antennas

A similar approximation to Hallén's equation can be carried out in the plane-wave case shown in Fig. 20.2.1. We distinguish three cases: (a) $Z_L = 0$, corresponding to a reflecting parasitic antenna with short-circuited output terminals, (b) $Z_L = \infty$, corresponding to open-circuited terminals, and (c) arbitrary Z_L , corresponding to a center-loaded receiving antenna. See Ref. [12] for more details on this approach.

By finding the short-circuit current from case (a) and the open-circuit voltage from case (b), we will determine the output impedance of the receiving antenna, that is, the Thévenin impedance Z_A of the model of Sec. 14.4, and show that it is equal to the input impedance (20.4.3) of the transmitting antenna, in accordance with the reciprocity principle. We will also show from case (c) that the angular gain pattern of the receiving antenna agrees with that of the transmitting one.

Starting with the short-circuited case, the approximation of Eq. (20.4.1) applied to (20.3.14) gives:

$$\bar{Z}I(z) = V(z) = C_1 e^{jkz} + C_2 e^{-jkz} + \frac{2E_0}{k \sin \theta} e^{jkz \cos \theta}$$

The end-point conditions $I(h) = I(-h) = 0$ provide two equations in the two unknowns C_1, C_2 , that is,

$$\begin{aligned} C_1 e^{jkh} + C_2 e^{-jkh} + \frac{2E_0}{k \sin \theta} e^{jkh \cos \theta} &= 0 \\ C_1 e^{-jkh} + C_2 e^{jkh} + \frac{2E_0}{k \sin \theta} e^{-jkh \cos \theta} &= 0 \end{aligned}$$

with solution:

$$C_1 = -\frac{E_0 \sin(kh(1 + \cos \theta))}{k \sin \theta \sin kh \cos kh}, \quad C_2 = -\frac{E_0 \sin(kh(1 - \cos \theta))}{k \sin \theta \sin kh \cos kh}$$

Then, the current $I(z)$ becomes:

$$I(z) = \frac{1}{Z} \left[C_1 e^{jkz} + C_2 e^{-jkz} + \frac{2E_0}{k \sin \theta} e^{jkz \cos \theta} \right] \quad (20.5.1)$$

For normal incidence, $\theta = 90^\circ$, we have $C_1 = C_2$ and Eq. (20.5.1) becomes:

$$I(z) = \frac{2E_0}{Zk \cos kh} (\cos kh - \cos kz) \quad (20.5.2)$$

For $\theta = 0$ and $\theta = \pi$, the z -component of the incident field is zero, $E_{in}(z) = 0$, and we expect $I(z) = 0$. This can be verified by carefully taking the limit of Eq. (20.5.1) at $\theta = 0, \pi$, with the seemingly diverging term $2E_0/k \sin \theta$ getting canceled.

The short-circuit current at the output terminals is obtained by setting $z = 0$ in Eq. (20.5.1):

$$I_{sc} = I(0) = \frac{1}{Z} \left[C_1 + C_2 + \frac{2E_0}{k \sin \theta} \right]$$

Inserting the expressions for C_1, C_2 , we find:

$$I_{sc} = \frac{2E_0}{Zk \cos kh} \frac{\cos kh - \cos(kh \cos \theta)}{\sin \theta} \quad (20.5.3)$$

For the open-circuit case, the incident field will induce an open-circuit voltage across the gap, and therefore, the scalar potential $\varphi(z)$ will be discontinuous at $z = 0$. In addition, the current must vanish at $z = 0$. Therefore, we must apply Eq. (20.3.14) separately to the upper and lower halves of the antenna. Using $\cos kz$ and $\sin kz$ as the homogeneous terms, instead of $e^{\pm jkz}$, we have the approximation:

$$\tilde{Z}I(z) = V(z) = \begin{cases} C_1 \cos kz + C_2 \sin kz + \frac{2E_0}{k \sin \theta} e^{jkz \cos \theta}, & z \geq 0 \\ D_1 \cos kz + D_2 \sin kz + \frac{2E_0}{k \sin \theta} e^{jkz \cos \theta}, & z \leq 0 \end{cases}$$

The conditions $I(0+) = I(h) = 0$ and $I(0-) = I(-h) = 0$ provide four equations in the four unknowns C_1, C_2, D_1, D_2 . They are:

$$\begin{aligned} C_1 + \frac{2E_0}{k \sin \theta} &= 0, & C_1 \cos kh + C_2 \sin kh + \frac{2E_0}{k \sin \theta} e^{jkh \cos \theta} &= 0 \\ D_1 + \frac{2E_0}{k \sin \theta} &= 0, & D_1 \cos kh - D_2 \sin kh + \frac{2E_0}{k \sin \theta} e^{-jkh \cos \theta} &= 0 \end{aligned}$$

with solution:

$$\begin{aligned} C_1 = D_1 &= -\frac{2E_0}{k \sin \theta} \\ C_2 &= \frac{2E_0 (\cos kh - e^{jkh \cos \theta})}{k \sin \theta \sin kh}, \quad D_2 = -\frac{2E_0 (\cos kh - e^{-jkh \cos \theta})}{k \sin \theta \sin kh} \end{aligned}$$

The open-circuit voltage is $V_{oc} = \varphi(0+) - \varphi(0-)$. Using Eq. (20.3.2), we have:

$$V'(0+) - V'(0-) = 2kV_{oc} = k(C_2 - D_2) \quad \Rightarrow \quad V_{oc} = \frac{1}{2}(C_2 - D_2)$$

and using the solution for C_2, D_2 , we find:

$$V_{oc} = \frac{2E_0}{k \sin kh} \frac{\cos kh - \cos(kh \cos \theta)}{\sin \theta} \quad (20.5.4)$$

Having found the short-circuit current and open-circuit voltage, we obtain the corresponding output Thévenin impedance by dividing Eq. (20.5.4) and (20.5.3):

$$Z_A = -\frac{V_{oc}}{I_{sc}} = -Z \cot kh \quad (20.5.5)$$

where the minus sign is due to the fact that I_{sc} is flowing into (instead of out of) the top antenna terminal. We note that Eq. (20.5.5) agrees with (20.4.3) of the transmitting case.

Equations (20.5.3) and (20.5.4) are special cases of a more general result, which is a consequence of the reciprocity principle (for example, see [35]). Given an incident field on a receiving linear antenna, the induced short-circuit current and open-circuit voltage at its terminals are given by:

$$I_{sc} = \frac{1}{V_0} \int_{-h}^h E_{in}(z) I(z) dz, \quad V_{oc} = -\frac{1}{I_0} \int_{-h}^h E_{in}(z) I(z) dz \quad (20.5.6)$$

where $I(z)$ is the current generated by V_0 when the antenna is transmitting. Inserting Eq. (20.4.2) into (20.5.6), we can easily derive Eqs. (20.5.3) and (20.5.4). We will use (20.5.6) in Sec. 21.2 to derive the mutual impedance between two antennas.

Finally, we consider case (c) of an arbitrary load impedance Z_L . The current will be continuous across the gap but it does not have to vanish at $z = 0$. The voltage difference across the gap will be equal to the voltage drop across the load, that is, $V_L = -Z_L I(0)$. The approximate Hallén equation is now:

$$\tilde{Z}I(z) = V(z) = \begin{cases} C_1 \cos kz + C_2 \sin kz + \frac{2E_0}{k \sin \theta} e^{jkz \cos \theta}, & z \geq 0 \\ D_1 \cos kz + D_2 \sin kz + \frac{2E_0}{k \sin \theta} e^{jkz \cos \theta}, & z \leq 0 \end{cases}$$

where $D_1 = C_1$ because of the continuity of $I(z)$ at $z = 0$. The end conditions, $I(h) = I(-h) = 0$, give:

$$\begin{aligned} C_1 \cos kh + C_2 \sin kh + \frac{2E_0}{k \sin \theta} e^{jkh \cos \theta} &= 0 \\ C_1 \cos kh - D_2 \sin kh + \frac{2E_0}{k \sin \theta} e^{-jkh \cos \theta} &= 0 \end{aligned}$$

Moreover, we have the discontinuity condition:

$$V'(0+) - V'(0-) = 2kV_L = k(C_2 - D_2) \quad \Rightarrow \quad V_L = \frac{1}{2}(C_2 - D_2)$$

Ohm's law at the load gives:

$$V_L = -Z_L I(0) = -\frac{Z_L}{Z} \left(C_1 + \frac{2E_0}{k \sin \theta} \right) = \frac{Z_L}{Z_A} \left(C_1 + \frac{2E_0}{k \sin \theta} \right) \cot kh$$

where we used Eq. (20.5.5). Solving the above four equations for C_1, C_2, D_2, V_L , we find eventually:

$$V_L = \frac{Z_L}{Z_A + Z_L} \frac{2E_0}{k \sin kh} \frac{\cos kh - \cos(kh \cos \theta)}{\sin \theta} = \frac{V_{oc} Z_L}{Z_A + Z_L} \quad (20.5.7)$$

This is equivalent to the Thévenin model that we used in Sec. 14.4. The power delivered to the load will be proportional to $|V_L|^2$, which is proportional to the gain pattern of a transmitting dipole, that is,

$$\left| \frac{\cos kh - \cos(kh \cos \theta)}{\sin \theta} \right|^2$$

20.6 King's Three-Term Approximation

To improve the crude sinusoidal approximation of Eq. (20.4.1), we must look more carefully at the properties of the impedance kernel. Separating its real and imaginary parts, we have:

$$Z(z - z') = \frac{j\eta}{2\pi} \frac{e^{-jkR}}{R} = \frac{k\eta}{2\pi} \left[\frac{\sin kR}{kR} + j \frac{\cos kR}{kR} \right]$$

For R near zero, the imaginary part becomes very large and we may apply the approximation (20.4.1) to it. But, the real part remains finite at $R = 0$. For $kR \leq \pi$, which will be guaranteed if $kh \leq \pi$, the sinc function can be very well approximated by $\cos(kR/2) \approx \cos(k|z - z'|/2)$ as can be verified by plotting the two functions. Therefore,

$$\frac{\sin kR}{kR} \approx \cos\left(\frac{kR}{2}\right) \approx \cos\left(\frac{k(z - z')}{2}\right), \quad \text{for } kR \leq \pi$$

Using this approximation for the real part of the kernel, and applying the approximation of Eq. (20.4.1) to its imaginary part, King has shown [4,75] that an improved approximation of the convolution integral is as follows:

$$\int_{-h}^h Z(z - z') I(z') dz' \approx R \cos\left(\frac{kz}{2}\right) + jXI(z)$$

where R, X are appropriate constants, which are real if $I(z)$ is real. This approximation also assumes that the current is symmetric, $I(z) = I(-z)$. Thus, Hallén's equation (20.3.13) can be approximated as:

$$R \cos\left(\frac{kz}{2}\right) + jXI(z) = V(z) = C_1 \cos kz + V_0 \sin k|z|$$

It shows that the current $I(z)$ is a linear combination of the sinusoidal terms $\sin k|z|$, $\cos kz$, and $\cos(kz/2)$. This leads to King's three-term approximation for the current [4,75], which incorporates the condition $I(h) = 0$. There are two alternative forms:

$$I(z) = A_1 I_1(z) + A_2 I_2(z) + A_3 I_3(z) = A'_1 I'_1(z) + A'_2 I'_2(z) + A'_3 I'_3(z) \quad (20.6.1)$$

where the expansion currents are defined by:

$$\begin{array}{l} I_1(z) = \sin k|z| - \sin kh \\ I_2(z) = \cos kz - \cos kh \\ I_3(z) = \cos(kz/2) - \cos(kh/2) \end{array}, \quad \begin{array}{l} I'_1(z) = \sin(k(h - |z|)) \\ I'_2(z) = \cos kz - \cos kh \\ I'_3(z) = \cos(kz/2) - \cos(kh/2) \end{array} \quad (20.6.2)$$

Using the trigonometric identity $I_1(z) = I'_2(z) \tan kh - I'_1(z) / \cos kh$, the relationship between the primed and unprimed coefficients is:

$$A'_1 = -\frac{A_1}{\cos kh}, \quad A'_2 = A_1 + A_2 \tan kh, \quad A'_3 = A_3 \quad (20.6.3)$$

The transformation between the primed and unprimed currents breaks down when $\cos kh = 0$, that is, when $l = 2h$ is an odd-multiple of $\lambda/2$. In that case, only the unprimed form may be used. Otherwise, the primed form is preferable because the term $I'_1(z) = \sin(k(h - |z|))$ has the conventional standing-wave form. We will work with the unprimed form because it is always possible.

To determine the expansion coefficients A_1, A_2, A_3 , we insert Eq. (20.6.1) into Hallén's equation (20.3.13) and get:

$$A_1 V_1(z) + A_2 V_2(z) + A_3 V_3(z) = V(z) = C_1 \cos kz + V_0 \sin k|z| \quad (20.6.4)$$

where

$$V_i(z) = \int_{-h}^h Z(z - z') I_i(z') dz', \quad i = 1, 2, 3 \quad (20.6.5)$$

At $z = h$, we have:

$$A_1 V_1(h) + A_2 V_2(h) + A_3 V_3(h) = V(h) = C_1 \cos kh + V_0 \sin kh \quad (20.6.6)$$

Subtracting Eqs. (20.6.4) and (20.6.6), and defining $V_{di}(z) = V_i(z) - V_i(h)$, we have:

$$A_1 V_{d1}(z) + A_2 V_{d2}(z) + A_3 V_{d3}(z) = C_1 (\cos kz - \cos kh) + V_0 (\sin k|z| - \sin kh)$$

Using the definition (20.6.2), we can write:

$$A_1 V_{d1}(z) + A_2 V_{d2}(z) + A_3 V_{d3}(z) = C_1 I_2(z) + V_0 I_1(z) \quad (20.6.7)$$

Introducing the difference kernel $Z_d(z - z') = Z(z - z') - Z(h - z')$, we have:

$$V_{di}(z) = \int_{-h}^h Z_d(z - z') I_i(z') dz', \quad i = 1, 2, 3 \quad (20.6.8)$$

The improved approximation applied to the difference kernel gives:

$$\int_{-h}^h Z_d(z-z')I(z')dz' = R(\cos(kz/2) - \cos(kh/2)) + jXI(z) = RI_3(z) + jXI(z)$$

Therefore, applying it to the three separate currents $I_1(z), I_2(z), I_3(z)$, we obtain:

$$V_{di}(z) = V_i(z) - V_i(h) = R_i I_3(z) + jX_i I_i(z), \quad i = 1, 2, 3 \quad (20.6.9)$$

Inserting these approximations in Eq. (20.6.4), we have:

$$A_1 [R_1 I_3(z) + jX_1 I_1(z)] + A_2 [R_2 I_3(z) + jX_2 I_2(z)] + A_3 [R_3 I_3(z) + jX_3 I_3(z)] = C_1 I_2(z) + V_0 I_1(z)$$

Defining $Z_3 = R_3 + jX_3$ and matching the coefficients of $I_1(z), I_2(z), I_3(z)$ in the two sides, gives three equations in the four unknowns A_1, A_2, A_3, C_1 :

$$jX_1 A_1 = V_0, \quad jX_2 A_2 - C_1 = 0, \quad R_1 A_1 + R_2 A_2 + Z_3 A_3 = 0$$

The fourth equation is (20.6.6). Thus, we obtain the linear system:

$$\begin{bmatrix} jX_1 & 0 & 0 & 0 \\ 0 & jX_2 & 0 & -1 \\ R_1 & R_2 & Z_3 & 0 \\ V_1(h) & V_2(h) & V_3(h) & -\cos kh \end{bmatrix} \begin{bmatrix} A_1 \\ A_2 \\ A_3 \\ C_1 \end{bmatrix} = \begin{bmatrix} V_0 \\ 0 \\ 0 \\ V_0 \sin kh \end{bmatrix} \quad (20.6.10)$$

The matrix elements can be determined by evaluating the defining approximations (20.6.9) at z -points at which the currents $I_i(z)$ take on their maximum values. For $I_1(z)$, the maximum occurs at $z_1 = 0$ if $h \leq \lambda/4$ and at $z_1 = h - \lambda/4$ if $\lambda/4 \leq h \leq 5\lambda/8$. For $I_2(z)$ and $I_3(z)$, the maxima occur at $z = 0$. Thus, the defining equations for the matrix elements are:

$$\begin{cases} V_{d1}(z_1) = V_1(z_1) - V_1(h) = R_1 I_3(z_1) + jX_1 I_1(z_1) \\ V_{d2}(0) = V_2(0) - V_2(h) = R_2 I_3(0) + jX_2 I_2(0) \\ V_{d3}(0) = V_3(0) - V_3(h) = Z_3 I_3(0) \end{cases} \quad (20.6.11)$$

The coefficients R_1, X_1, R_2, X_2 are obtained by extracting the real and imaginary parts of these expressions. The left-hand sides can be computed by direct numerical integration of the definitions (20.6.5). The expected range of applicability of the 3-term approximation is for antenna lengths $l \leq 1.25\lambda$ (see [4,75].) However, it works well even for longer lengths.

The MATLAB function `king` implements the design equations (20.6.10) and (20.6.11). It has usage:

```
A = king(L,a); % King's 3-term sinusoidal approximation
```

where L, a are the antenna length and its radius in units of λ and the output A is the column vector of the coefficients A_i . If the length is an odd-multiple of $\lambda/2$, then $A = [A_1, A_2, A_3]^T$, otherwise, $A = [A'_1, A'_2, A'_3]^T$.

The numerical integrations are done with a 32-point Gauss-Legendre quadrature integration routine implemented with the function `quadr`, which provides the appropriate weights and evaluation points for the integration.

Example 20.6.1: Fig. 20.6.1 compares the three-term approximation to the standard sinusoidal approximation, $I(z) = \sin(k(h - |z|))$, and to the exact numerical solution of Hallén's equation for the two cases of $l = \lambda$ and $l = 1.5\lambda$. The antenna radius was $a = 0.005\lambda$.

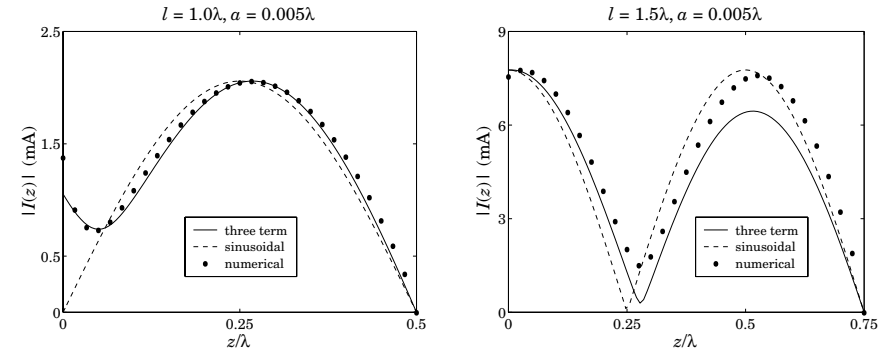


Fig. 20.6.1 Three-term approximation for $l = \lambda$ and $l = 1.5\lambda$.

In the full-wavelength case, the sinusoidal approximation has $I(0) = 0$, which would imply infinite antenna impedance. The three-term approximation gives a nonzero value for $I(0)$. The computed three-term coefficients are in the two cases:

$$\begin{bmatrix} A'_1 \\ A'_2 \\ A'_3 \end{bmatrix} = 10^{-3} \begin{bmatrix} -3.0409j \\ 0.3573 + 0.3686j \\ 0.3044 + 0.3369j \end{bmatrix}, \quad \begin{bmatrix} A_1 \\ A_2 \\ A_3 \end{bmatrix} = 10^{-3} \begin{bmatrix} -2.4348j \\ 7.8154 - 3.6654j \\ 0.9416 + 2.8503j \end{bmatrix}$$

We used the primed representation of Eq. (20.6.1) for the full-wavelength case, and the unprimed one for $l = 1.5\lambda$. The graphs were generated by the following example code:

```
L = 1.0; % length in wavelengths
a = 0.008; % radius in wavelengths
h = L/2;
k = 2*pi; % wavenumber in rads/wavelength

A = king(L,a); % 3-term coefficients
z = 0 : h/100 : h;
Ik = kingeval(L,A,z); % evaluate 3-term approximation
Is = sin(k*(h-abs(z))); % sinusoidal approximation

M = 30; % number of upper-half segments
[In,zn,cnd] = hallen(L,a,M); % numerical solution
In = In(M+1:end); % upper-half of the current
zn = zn(M+1:end); % centers of upper-half segments

mk = max(abs(Ik)); % scale factors
ms = max(abs(Is));
mn = max(abs(In));

plot(z, abs(Ik)*mn/mk, z, abs(Is)*mn/ms, '--', zn, abs(In), '.');
```

The function `kingeval` simply evaluates the three-term approximation (20.6.1) at a given number of z -points. □

20.7 Numerical Solution of Hallén's Equation

In the past three sections, we looked at approximate solutions of Hallén's equation obtained by simplifying the convolution integral.

Here, we discuss numerical solutions of the full integral equation based on moment methods. We consider both the delta-gap case of a center-driven antenna and the more general case of an arbitrary incident field. The relevant Hallén equations are Eqs. (20.3.12) and (20.3.13), that is,

$$\int_{-h}^h Z(z-z')I(z')dz' = V(z) = C_1 \cos kz + V_0 \sin k|z| \quad (20.7.1)$$

$$\int_{-h}^h Z(z-z')I(z')dz' = V(z) = C_1 e^{jkz} + C_2 e^{-jkz} + \int_{-h}^h F(z-z')E_{in}(z')dz' \quad (20.7.2)$$

A numerical solution attempts to discretize these equations and convert them to a system of linear equations. Perhaps, the simplest scheme is to replace the current $I(z)$ by its sampled version, sampled at $N = 2M + 1$ equally-spaced z -points along the antenna length, that is,

$$I(z') = \sum_{m=-M}^M I(z_m) \delta(z' - z_m) \Delta z \quad (20.7.3)$$

where for $-M \leq m \leq M$,

$$z_m = m\Delta z, \quad \Delta z = \frac{h}{M} = \frac{l}{N-1} \quad (\text{type-0}) \quad (20.7.4)$$

Such a discretization scheme is shown on the lower part of Fig. 20.7.1, labeled as "type-0", for the case of $N = 11$ and $M = 5$. The spacing interval Δz appears as a factor in Eq. (20.7.3) in order to have the right dimensions for $I(z)$. Note that the last sample coincides with the end-point of the antenna, $z_M = M\Delta z = h$. The antenna length is divided into $N - 1$ segments of length Δz and two half-segments of length $\Delta z/2$ at the two ends.

The sharp delta function $\delta(z - z_m) \Delta z$ can be replaced by a finite pulse of width Δz centered around the point z_m , as shown in Fig. 20.7.1. We will consider this case later. Inserting Eq. (20.7.3) into (20.7.1), the integration can be done trivially giving:

$$\sum_{m=-M}^M Z(z - z_m)I(z_m)\Delta z = V(z) = C_1 \cos kz + V_0 \sin k|z|$$

If we evaluate this equation at the same sampled points $z_n = n\Delta z$, we will obtain an $N \times N$ system of linear equations in the unknowns $I(z_m)$, that is,

$$\sum_{m=-M}^M Z(z_n - z_m)I(z_m)\Delta z = V(z_n) = C_1 \cos kz_n + V_0 \sin k|z_n| \quad (20.7.5)$$

for $-M \leq n \leq M$. The constant C_1 will be chosen in order to satisfy the end condition $I(z_M) = I(h) = 0$. Eq. (20.7.5) can be written in the compact matrix form:

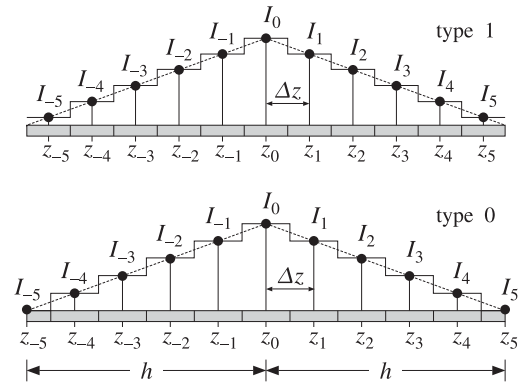


Fig. 20.7.1 Sampling schemes along an antenna, with $N = 11$, $M = 5$.

$$\mathbf{Z}\mathbf{I} = \mathbf{v} = \mathbf{C}_1\mathbf{c} + V_0\mathbf{s} \quad (20.7.6)$$

where \mathbf{Z} is the $N \times N$ matrix $Z_{nm} = Z(z_n - z_m) \Delta z$ and \mathbf{I} , \mathbf{s} , and \mathbf{c} are the column vectors with elements $I_n = I(z_n)$, $c_n = \cos kz_n$, and $s_n = \sin k|z_n|$, and $v_n = C_1 c_n + V_0 s_n$, for $n = -M, \dots, M$. All of these vectors are symmetric about their middle, that is, $I(z_{-n}) = I(z_n)$, and similarly for the others. Therefore, we have:

$$\mathbf{I} = \begin{bmatrix} I_M \\ \vdots \\ I_1 \\ I_0 \\ I_1 \\ \vdots \\ I_M \end{bmatrix}, \quad \mathbf{v} = \begin{bmatrix} v_M \\ \vdots \\ v_1 \\ v_0 \\ v_1 \\ \vdots \\ v_M \end{bmatrix}, \quad \mathbf{c} = \begin{bmatrix} c_M \\ \vdots \\ c_1 \\ c_0 \\ c_1 \\ \vdots \\ c_M \end{bmatrix}, \quad \mathbf{s} = \begin{bmatrix} s_M \\ \vdots \\ s_1 \\ s_0 \\ s_1 \\ \vdots \\ s_M \end{bmatrix} \quad (20.7.7)$$

The matrix \mathbf{Z} is a symmetric Toeplitz matrix because the nm th matrix element depends only on the difference $|n - m|$, indeed,

$$Z_{nm} = Z(z_n - z_m) \Delta z = \Delta z \frac{j\eta}{2\pi} \frac{e^{-jkR}}{R}, \quad R = \sqrt{a^2 + \Delta z^2 (n - m)^2} \quad (20.7.8)$$

Taking advantage of the Toeplitz nature of \mathbf{Z} and the symmetry of the vectors (20.7.7), the matrix system (20.7.6) can be replaced by one essentially half its size, thus, speeding up the solution. To see this, we partition the vector \mathbf{I} into its upper (negative- z), middle, and lower (positive- z) parts:

$$\mathbf{I} = \begin{bmatrix} \mathbf{I}_1^R \\ I_0 \\ \mathbf{I}_1 \end{bmatrix}, \quad \mathbf{I}_1 = \begin{bmatrix} I_1 \\ I_2 \\ \vdots \\ I_M \end{bmatrix}, \quad \mathbf{I}_1^R = \begin{bmatrix} I_M \\ \vdots \\ I_2 \\ I_1 \end{bmatrix}$$

The upper part I_1^R is the *reverse* of the lower part I_1 . The reversal operation can be expressed as a matrix operation:

$$I_1^R = JI_1, \quad J = \begin{bmatrix} 0 & \cdots & 0 & 1 \\ 0 & \cdots & 1 & 0 \\ \vdots & \ddots & \vdots & \vdots \\ 1 & \cdots & 0 & 0 \end{bmatrix}$$

where J is the $M \times M$ reversing matrix J , that is, the matrix with ones along its antidiagonal. Then, the impedance matrix Z and Eq. (20.7.6) can be partitioned in a compatible way as follows:

$$\begin{bmatrix} A^R & \mathbf{a}_1^R & B^R \\ \mathbf{a}_2^{TR} & a_0 & \mathbf{a}_2^T \\ B & \mathbf{a}_1 & A \end{bmatrix} \begin{bmatrix} I_1^R \\ I_0 \\ I_1 \end{bmatrix} = \begin{bmatrix} \mathbf{v}_1^R \\ v_0 \\ \mathbf{v}_1 \end{bmatrix} \quad (20.7.9)$$

where we have separated out the middle column and row of Z . Because Z satisfies the reversal invariance condition $Z(n, m) = Z(-n, -m)$, the upper-left block A^R will be the reverse of the lower-right block A , and the upper-right, the reverse of the lower-left. Moreover, because Z is symmetric, we have $\mathbf{a}_2 = \mathbf{a}_1$, and also for the Toeplitz submatrices, $A^R = A^T = A$ and $B^R = B^T$.

The reverse of a matrix is obtained by reversing its columns and then reversing its rows, an operation which is equivalent to multiplication by the reversing matrix J from left and right:

$$A^R = JAJ$$

Writing out the three sub-block equations of Eq. (20.7.9), we obtain:

$$\begin{aligned} A^R I_1^R + \mathbf{a}_1^R I_0 + B^R I_1 &= \mathbf{v}_1^R \\ \mathbf{a}_2^{TR} I_1^R + a_0 I_0 + \mathbf{a}_2^T I_1 &= v_0 \\ B I_1^R + \mathbf{a}_1 I_0 + A I_1 &= \mathbf{v}_1 \end{aligned}$$

But, the first is exactly the reverse of the last, and therefore redundant. Noting that $\mathbf{a}_2^{TR} I_1^R = \mathbf{a}_2^T I_1$ and $B I_1^R = B J I_1$, we obtain the reduced system:

$$\begin{aligned} a_0 I_0 + 2\mathbf{a}_2^T I_1 &= v_0 \\ \mathbf{a}_1 I_0 + (A + B J) I_1 &= \mathbf{v}_1 \end{aligned}$$

which can be written in the reduced block matrix form:

$$\begin{bmatrix} a_0 & 2\mathbf{a}_2^T \\ \mathbf{a}_1 & A + B J \end{bmatrix} \begin{bmatrix} I_0 \\ I_1 \end{bmatrix} = \begin{bmatrix} v_0 \\ \mathbf{v}_1 \end{bmatrix} \quad (20.7.10)$$

Thus, we can replace the $N \times N$ system (20.7.6) or (20.7.9) by the $(M+1) \times (M+1)$ system (20.7.10) acting only on half-vectors. We will write Eq. (20.7.10) in the following compact form:

$$\boxed{ZI = \mathbf{v} = C_1 \mathbf{c} + V_0 \mathbf{s}} \quad (20.7.11)$$

where Z is constructed from \tilde{Z} according to (20.7.10) and the vectors are the half-vectors:

$$I = \begin{bmatrix} I_0 \\ I_1 \\ \vdots \\ I_M \end{bmatrix}, \quad \mathbf{v} = \begin{bmatrix} v_0 \\ v_1 \\ \vdots \\ v_M \end{bmatrix}, \quad \mathbf{c} = \begin{bmatrix} c_0 \\ c_1 \\ \vdots \\ c_M \end{bmatrix}, \quad \mathbf{s} = \begin{bmatrix} s_0 \\ s_1 \\ \vdots \\ s_M \end{bmatrix} \quad (20.7.12)$$

Next, we impose the condition that $I_M = 0$. It can be written vectorially in the form $\mathbf{u}^T I = 0$, where $\mathbf{u}^T = [0, \dots, 0, 1]$. Solving (20.7.11) for I , we obtain:

$$\boxed{I = C_1 Z^{-1} \mathbf{c} + V_0 Z^{-1} \mathbf{s}} \quad (20.7.13)$$

Multiplying both sides by \mathbf{u}^T , we obtain the condition:

$$\mathbf{u}^T I = C_1 \mathbf{u}^T Z^{-1} \mathbf{c} + V_0 \mathbf{u}^T Z^{-1} \mathbf{s} = 0$$

which may be solved for C_1 :

$$\boxed{C_1 = -V_0 \frac{\mathbf{u}^T Z^{-1} \mathbf{s}}{\mathbf{u}^T Z^{-1} \mathbf{c}}} \quad (20.7.14)$$

The two equations (20.7.13) and (20.7.14) provide the complete solution of the discretized Hallén equation. The MATLAB function `hallen` implements this solution procedure. It has usage:

```
[I, z, cnd] = hallen(L, a, M); % solve Hallen's integral equation with delta-gap input
```

The function solves the half system (20.7.11) but returns the full N -dimensional symmetric vector I of Eq. (20.7.7). The quantity \mathbf{z} is the N -dimensional vector of sampled z -points (20.7.4), and `cnd` is the condition number of the matrix Z that is being inverted. The quantities L, a are the antenna length and radius in units of λ , and M has the same meaning as above. It assumes $V_0 = 1$. Therefore, the input impedance of the antenna will be $Z_A = V_0/I_0 = 1/I_0$.

Because the submatrices A, B in (20.7.10) are Toeplitz, it follows that the row-reversed matrix $B J$ will be Hankel. These matrices are constructed with the help of the MATLAB functions `toeplitz` and `hankel`. No inverse of Z is computed. Instead we perform the single MATLAB operation $Z \setminus [\mathbf{c}, \mathbf{s}]$, from which the rest of the solution can be constructed.

Fast Toeplitz solvers can also be used, based on the Levinson recursion and fast Cholesky factorizations [52]. However, we found that the built-in linear system solver of MATLAB is much faster for sizes of the order $M = 20$ -100.

20.8 Numerical Solution Using Pulse Functions

The delta function discretization scheme works well. An example was seen in Fig. 20.6.1. An alternative to this discretization is to replace the delta functions with finite pulses of width Δz , that is,

$$\delta(z - z_m) \Delta z \rightarrow \Delta(z - z_m)$$

where $\Delta(z)$ is the unit-pulse centered at the origin:

$$\Delta(z) = u(z + \Delta z/2) - u(z - \Delta z/2) = \begin{cases} 1, & \text{if } |z| \leq \frac{1}{2}\Delta z \\ 0, & \text{otherwise} \end{cases} \quad (20.8.1)$$

The delta function is obtained in the limit $\Delta z \rightarrow 0$:

$$\delta(z) = \lim_{\Delta z \rightarrow 0} \frac{\Delta(z)}{\Delta z}$$

The sampled current (20.7.3) is now replaced by:

$$I(z') = \sum_{m=-M}^M I(z_m) \Delta(z' - z_m) \quad (20.8.2)$$

and Hallén's equation becomes:

$$\sum_{m=-M}^M I(z_m) \int_{-h}^h Z(z - z') \Delta(z' - z_m) dz' = V(z) = C_1 \cos kz + V_0 \sin k|z|$$

Evaluating it at the sampled points $z_n = n\Delta z$, for $-M \leq n \leq M$, we have:

$$\sum_{m=-M}^M I(z_m) \int_{-h}^h Z(z_n - z') \Delta(z' - z_m) dz' = V(z_n) = C_1 \cos kz_n + V_0 \sin k|z_n|$$

We define the impedance matrix by:

$$Z_{nm} = \int_{-h}^h Z(z_n - z') \Delta(z' - z_m) dz' \quad (20.8.3)$$

Changing variable of integration to $z'' = z' - z_m$, and noting that $\Delta(z'')$ has unity height and support on the Δz -interval centered at the origin, the above integration range reduces to:[†]

$$Z_{nm} = \int_{-\Delta z/2}^{\Delta z/2} Z(z_n - z_m - z'') \Delta(z'') dz'' = \int_{-\Delta z/2}^{\Delta z/2} Z(z_n - z_m - z'') dz''$$

Changing variables again to $z'' = x\Delta z$, we have the final form of the matrix:

$$Z_{nm} = \Delta z \int_{-1/2}^{1/2} Z(z_n - z_m - x\Delta z) dx \quad (20.8.4)$$

where

$$Z(z_n - z_m - x\Delta z) = \frac{j\eta}{2\pi} \frac{e^{-jkR}}{R}, \quad R = \sqrt{a^2 + \Delta z^2(n - m - x)^2}$$

The resulting discrete Hallén equation becomes:

[†]Strictly speaking, at the two ends of the antenna, the z'' segment is only half as long as the other segments. However, very little loss of accuracy arises if we artificially extend these end-segments to full length Δz . This issue does not arise in the type-1 case.

$$\sum_{m=-M}^M Z_{nm} I_m = V(z_n) = C_1 \cos kz_n + V_0 \sin k|z_n| \quad (20.8.5)$$

and can be written in a similar matrix form as (20.7.6):

$$Z\mathbf{I} = \mathbf{v} = C_1\mathbf{c} + V_0\mathbf{s} \quad (20.8.6)$$

The only difference between this and (20.7.6) is in the definition of the sampled impedance matrix Z . In this case too, Z is Toeplitz, symmetric, and invariant under reversal. Therefore, it can be wrapped to half-size in exactly the same fashion as Eq. (20.7.11).

The MATLAB function `hallen` also implements this case. The required integration over x is done using Gauss-Legendre quadrature integration with N_{int} points. The MATLAB function `quadr` is used to provide the N_{int} weights and evaluation points:

$$[w, x] = \text{quadr}(-1/2, 1/2, N_{\text{int}});$$

The integral in (20.8.4) is then calculated by the dot product:

$$Z_{nm} = \mathbf{w}^T Z(z_n - z_m - \mathbf{x}\Delta z) \Delta z \quad (20.8.7)$$

where $Z(z_n - z_m - \mathbf{x}\Delta z)$ is the column vector of values of the integrand at the Gauss-Legendre evaluation points \mathbf{x} . Some examples of weights and evaluation points are given below for $N_{\text{int}} = 1, 2, 3$:

$$\begin{aligned} \mathbf{w} &= [1], & \mathbf{w} &= \begin{bmatrix} 0.5000 \\ 0.5000 \end{bmatrix}, & \mathbf{w} &= \begin{bmatrix} 0.2778 \\ 0.4444 \\ 0.2778 \end{bmatrix} \\ \mathbf{x} &= [0], & \mathbf{x} &= \begin{bmatrix} -0.2887 \\ 0.2887 \end{bmatrix}, & \mathbf{x} &= \begin{bmatrix} -0.3873 \\ 0.0000 \\ 0.3873 \end{bmatrix} \end{aligned}$$

We note in particular, that the case $N_{\text{int}} = 1$ has unity weight and evaluation point $x = 0$ so that Eq. (20.8.7) becomes identical to (20.7.8). Thus, the delta-function case is obtained as a special case of our implementation of the pulse case. The function `hallen` can be called with an extra input parameter to specify the number of integration points:

$$[I, z, \text{cnd}] = \text{hallen}(L, a, M, N_{\text{int}}); \quad \% \text{Hallén's integral equation with delta-gap input}$$

The function also has an additional optional input variable, `type`, which takes on the values 0, 1 and specifies the desired sampling scheme, as shown in Fig. 20.7.1. Thus, the full set of input parameters of the function is:

$$[I, z, \text{cnd}] = \text{hallen}(L, a, M, N_{\text{int}}, \text{type}); \quad \% \text{Hallén's integral equation with delta-gap input}$$

The type-1 case corresponds to dividing the antenna into $N = 2M + 1$ equal sub-intervals, instead of the $(N - 1)$ of the type-0 case. Now, the sampling points are defined as follows, for $-M \leq m \leq M$,

$$z_m = m\Delta z, \quad \Delta z = \frac{h}{M + 0.5} = \frac{l}{N} \quad (\text{type-1}) \quad (20.8.8)$$

The last sample does not quite reach the end of the antenna, $z_M = M\Delta z = h - \Delta z/2$. However, our solution still enforces the end-point condition $I(z_M) = 0$. This can be justified by thinking of $I(z_M)$ as representing the value of entire last pulse interval, which does extend to the end of the antenna.

Example 20.8.1: To clarify the structure of the impedance matrix (20.8.4) and show how to wrap it efficiently into the half-size of (20.7.10), consider the case $N = 7$ or $M = 3$. Because Z is Toeplitz and symmetric, it can be built from the knowledge of its first column or first row. The first row is $Z_{n,-M} = Z_{n+M,0}$, for $-M \leq n \leq M$. Setting $m = n + M$, so that $m = 0, 1, \dots, 2M$, the first row consists of the numbers:

$$a_m = \Delta z \frac{j\eta}{2\pi} \int_{-1/2}^{1/2} \frac{e^{-jkR}}{R} dx, \quad R = \sqrt{a^2 + \Delta z^2 (m-x)^2} \quad (20.8.9)$$

Therefore, the full matrix Z will have the form:

$$Z = \begin{array}{c|ccc|ccc} \begin{array}{c} a_0 \\ a_1 \\ a_2 \\ a_3 \\ a_4 \\ a_5 \\ a_6 \end{array} & \begin{array}{c} a_1 \\ a_0 \\ a_1 \\ a_2 \\ a_3 \\ a_4 \\ a_5 \end{array} & \begin{array}{c} a_2 \\ a_1 \\ a_0 \\ a_2 \\ a_3 \\ a_4 \\ a_5 \end{array} & \begin{array}{c} a_3 \\ a_2 \\ a_1 \\ a_0 \\ a_2 \\ a_3 \\ a_4 \end{array} & \begin{array}{c} a_4 \\ a_3 \\ a_2 \\ a_1 \\ a_0 \\ a_2 \\ a_3 \end{array} & \begin{array}{c} a_5 \\ a_4 \\ a_3 \\ a_2 \\ a_1 \\ a_0 \\ a_2 \end{array} & \begin{array}{c} a_6 \\ a_5 \\ a_4 \\ a_3 \\ a_2 \\ a_1 \\ a_0 \end{array} \\ \hline \begin{array}{c} a_0 \\ a_1 \\ a_2 \\ a_3 \\ a_4 \\ a_5 \\ a_6 \end{array} & \begin{array}{c} a_1 \\ a_0 \\ a_1 \\ a_2 \\ a_3 \\ a_4 \\ a_5 \end{array} & \begin{array}{c} a_2 \\ a_1 \\ a_0 \\ a_2 \\ a_3 \\ a_4 \\ a_5 \end{array} & \begin{array}{c} a_3 \\ a_2 \\ a_1 \\ a_0 \\ a_2 \\ a_3 \\ a_4 \end{array} & \begin{array}{c} a_4 \\ a_3 \\ a_2 \\ a_1 \\ a_0 \\ a_2 \\ a_3 \end{array} & \begin{array}{c} a_5 \\ a_4 \\ a_3 \\ a_2 \\ a_1 \\ a_0 \\ a_2 \end{array} & \begin{array}{c} a_6 \\ a_5 \\ a_4 \\ a_3 \\ a_2 \\ a_1 \\ a_0 \end{array} \end{array}$$

where we partitioned it as in Eq. (20.7.10), with submatrices:

$$A = \begin{bmatrix} a_0 & a_1 & a_2 \\ a_1 & a_0 & a_1 \\ a_2 & a_1 & a_0 \end{bmatrix}, \quad B = \begin{bmatrix} a_4 & a_3 & a_2 \\ a_5 & a_4 & a_3 \\ a_6 & a_5 & a_4 \end{bmatrix}, \quad \mathbf{a}_1 = \mathbf{a}_2 = \begin{bmatrix} a_1 \\ a_2 \\ a_3 \end{bmatrix}$$

Therefore, the wrapped version of Z will be:

$$Z = \begin{bmatrix} a_0 & 2\mathbf{a}_1^T \\ \mathbf{a}_1 & A + BJ \end{bmatrix} = \begin{bmatrix} a_0 & 2a_1 & 2a_2 & 2a_3 \\ a_1 & a_0 + a_2 & a_1 + a_3 & a_2 + a_4 \\ a_2 & a_1 + a_3 & a_0 + a_4 & a_1 + a_5 \\ a_3 & a_2 + a_4 & a_1 + a_5 & a_0 + a_6 \end{bmatrix} \quad (20.8.10)$$

This matrix can be constructed quickly as follows. Once the numbers a_m , $m = 0, 1, \dots, 2M$ are computed, take the first and last $M + 1$ numbers, that is, define the two row vectors \mathbf{a}_t , \mathbf{a}_h :

$$\mathbf{a} = [a_0, a_1, a_2, a_3, a_4, a_5, a_6] \Rightarrow \mathbf{a}_t = [a_0, a_1, a_2, a_3], \quad \mathbf{a}_h = [a_3, a_4, a_5, a_6]$$

Then, form the Toeplitz matrix whose first column and first row are \mathbf{a}_t , and add it to the Hankel matrix whose first column is \mathbf{a}_t and last row is \mathbf{a}_h . This is accomplished easily by the built-in MATLAB functions `toeplitz` and `hankel`:

$$\text{toeplitz}(\mathbf{a}_t, \mathbf{a}_t) + \text{hankel}(\mathbf{a}_t, \mathbf{a}_h) = \begin{bmatrix} 2a_0 & 2a_1 & 2a_2 & 2a_3 \\ 2a_1 & a_0 + a_2 & a_1 + a_3 & a_2 + a_4 \\ 2a_2 & a_1 + a_3 & a_0 + a_4 & a_1 + a_5 \\ 2a_3 & a_2 + a_4 & a_1 + a_5 & a_0 + a_6 \end{bmatrix}$$

Then, replace the first column by half its value. These procedures are incorporated into the function `hallen`. \square

Example 20.8.2: Another numerical issue is the accuracy of the Gauss-Legendre integration. The accuracy can be improved by increasing N_{int} (typical values are 16–32.) But a better method is to keep N_{int} fixed at some value, say 16, and split the integration interval into several subintervals, for example,

$$\int_{-1/2}^{1/2} = \int_{-1/2}^{-\delta} + \int_{-\delta}^{\delta} + \int_{\delta}^{1/2}$$

Then, compute the Legendre weights and evaluation points in each subinterval:

$$\begin{aligned} [\mathbf{w1}, \mathbf{x1}] &= \text{quadr}(-1/2, -\delta, N_{\text{int}}); \\ [\mathbf{w2}, \mathbf{x2}] &= \text{quadr}(-\delta, \delta, N_{\text{int}}); \\ [\mathbf{w3}, \mathbf{x3}] &= \text{quadr}(\delta, 1/2, N_{\text{int}}); \end{aligned}$$

And, finally, add the values of the sub-integrals. This procedure is not implemented into `hallen`, but is implemented into the `king` function and also into `imped`, which calculates the self and mutual impedance of dipole antennas. \square

20.9 Numerical Solution for Arbitrary Incident Field

The numerical solution of Hallén's equation with arbitrary incident field, Eq. (20.7.2), can be accomplished in the same way as in the delta-gap case. Assuming a pulse basis expansion for both the current and the incident field, we have:

$$\begin{aligned} I(z') &= \sum_{m=-M}^M I(z_m) \Delta(z' - z_m) \\ E_{\text{in}}(z') &= \sum_{m=-M}^M E_{\text{in}}(z_m) \Delta(z' - z_m) \end{aligned} \quad (20.9.1)$$

Sampled at the points $z_n = n\Delta z$, $-M \leq n \leq M$, the convolution of the incident field with the Green's function $F(z)$ becomes:

$$\int_{-h}^h F(z_n - z') E_{\text{in}}(z') dz' = \sum_{m=-M}^M E_{\text{in}}(z_m) \int_{-h}^h F(z_n - z') \Delta(z' - z_m) dz'$$

As in Eq. (20.8.3), we define the Green's matrix:

$$F_{nm} = \int_{-h}^h F(z_n - z') \Delta(z' - z_m) dz' \quad (20.9.2)$$

Changing integration variable to $z' = z_m + \alpha\Delta z$, we may rewrite this as:

$$F_{nm} = \Delta z \int_{-1/2}^{1/2} F(z_n - z_m - \alpha\Delta z) d\alpha \quad (20.9.3)$$

And, in particular, if we use $F(z) = je^{-jk|z|}$ as the Green's function:

$$F_{nm} = \Delta z \int_{-1/2}^{1/2} je^{-jk\Delta z|n-m-\alpha|} d\alpha \quad (20.9.4)$$

The integration can be done exactly giving the matrix elements:

$$F_{nm} = \Delta z \left[\frac{1 - \cos(k\Delta z/2)}{k\Delta z/2} \delta_{nm} + \frac{\sin(k\Delta z/2)}{k\Delta z/2} je^{-jk\Delta z|n-m|} \right] \quad (20.9.5)$$

The discretized Hallén equation (20.7.2) then takes the form:

$$\sum_{m=-M}^M Z_{nm} I_m = C_1 e^{jkz_n} + C_2 e^{-jkz_n} + \sum_{m=-M}^M F_{nm} E_m \quad (20.9.6)$$

where we denoted $E_m = E_{in}(z_m)$. Eq. (20.9.6) can be written in the compact form:

$$\mathbf{Z}\mathbf{I} = C_1 \mathbf{s}_1 + C_2 \mathbf{s}_2 + \mathbf{F}\mathbf{E} \quad (20.9.7)$$

where \mathbf{s}_1 and \mathbf{s}_2 are the vectors with elements $s_1(n) = e^{jkz_n}$ and $s_2(n) = e^{-jkz_n}$. Defining the $N \times 2$ matrix $S = [\mathbf{s}_1, \mathbf{s}_2]$ and the two-dimensional column vector of constants $\mathbf{C} = [C_1, C_2]^T$, we write Eq. (20.9.7) in the form:

$$\mathbf{Z}\mathbf{I} = \mathbf{S}\mathbf{C} + \mathbf{F}\mathbf{E} \quad (20.9.8)$$

It is not possible to wrap this equation in half because \mathbf{E} is not necessarily symmetric about its middle. The constants \mathbf{C} must be found by imposing the two independent end conditions $I(z_M) = I(-z_M) = 0$. These conditions can be written compactly as:

$$U^T \mathbf{I} = \mathbf{0}$$

where $U = [\mathbf{u}_{top}, \mathbf{u}_{bot}]$ and $\mathbf{u}_{top} = [1, 0, \dots, 0]^T$ selects the top entry of the vector \mathbf{I} , while $\mathbf{u}_{bot} = [0, \dots, 0, 1]^T$ selects the bottom entry. Solving for \mathbf{I} , we have:

$$\mathbf{I} = \mathbf{Z}^{-1} \mathbf{S}\mathbf{C} + \mathbf{Z}^{-1} \mathbf{F}\mathbf{E} \quad (20.9.9)$$

Multiplying from the left by the matrix U^T , we obtain the condition:

$$U^T \mathbf{I} = U^T \mathbf{Z}^{-1} \mathbf{S}\mathbf{C} + U^T \mathbf{Z}^{-1} \mathbf{F}\mathbf{E} = \mathbf{0}$$

which may be solved for \mathbf{C} :

$$\mathbf{C} = - (U^T \mathbf{Z}^{-1} \mathbf{S})^{-1} (U^T \mathbf{Z}^{-1} \mathbf{F}) \mathbf{E} \quad (20.9.10)$$

The two equations (20.9.9) and (20.9.10) describe the complete solution of the discrete Hallén equation (20.9.8). The MATLAB function `hallen2` implements this solution procedure. Its usage is:

```
[I, z, cnd] = hallen2(L, a, E, Nint, type); % Hallen's equation with arbitrary incident E-field
```

where instead of the parameter M , it has as input the vector \mathbf{E} of the samples of the incident field. The dimension $N = 2M + 1$ is extracted from the length of \mathbf{E} . The default values of the last two input parameters are $N_{int} = 16$ and `type = 1`.

The functions `hallen` and `hallen2` produce practically identical output in the delta-gap case, that is, when the incident field is:

$$\mathbf{E} = \underbrace{[0, 0, \dots, 0]}_{M \text{ zeros}}, \frac{1}{\Delta z}, \underbrace{[0, \dots, 0, 0]}_{M \text{ zeros}}]^T \quad (20.9.11)$$

The middle entry imitates the delta-gap $V_0 \delta(z) \approx V_0 \Delta(z) / \Delta z = V_0 / \Delta z$. For the case of a field incident at a polar angle θ as in Eq. (20.2.3), the sampled vector \mathbf{E} will have entries, for $-M \leq n \leq M$:

$$E_n = E_0 \sin \theta e^{jkz_n \cos \theta} \quad (20.9.12)$$

20.10 Numerical Solution of Pocklington's Equation

Pocklington's equation (20.1.10) is an alternative equation for determining the current $I(z)$ induced by a given incident field $E_{in}(z)$. It can be solved numerically by similar discretization techniques as in the previous section. Rearranging the constants in Eq. (20.1.10), we can write it in the form:

$$\int_{-h}^h I(z') Z(z - z') dz' = E_{in}(z) \quad (20.10.1)$$

where we defined the Pocklington impedance kernel by:

$$Z(z - z') = \frac{j\eta\lambda}{8\pi^2} (\partial_z^2 + k^2) G(z - z') \quad (20.10.2)$$

Assuming a pulse function expansion of the type of Eq. (20.8.2) and evaluating (20.10.1) at the sampling points $z_n = n\Delta z$, we obtain the discretized version:

$$\sum_{m=-M}^M I(z_m) \int_{-h}^h Z(z_n - z') \Delta(z' - z_m) dz' = E(z_n) \quad (20.10.3)$$

As before, we define the impedance matrix (it has units of ohm/m):

$$Z_{nm} = \int_{-h}^h Z(z_n - z') \Delta(z' - z_m) dz' = \int_{-\Delta z/2}^{\Delta z/2} Z(z_n - z_m - z'') dz'' \quad (20.10.4)$$

Part of this integral can be done directly, with no approximations. We have:

$$Z_{nm} = \frac{j\eta\lambda}{8\pi^2} \int_{-\Delta z/2}^{\Delta z/2} (\partial_{z''}^2 + k^2) G(z_n - z_m - z'') dz''$$

where we replaced ∂_z^2 by $\partial_{z''}^2$. Integrating the first term, we obtain:

$$Z_{nm} = \frac{j\eta\lambda}{8\pi^2} \left[\partial_{z''} G(R_+) - \partial_{z''} G(R_-) + k^2 \int_{-\Delta z/2}^{\Delta z/2} G(z_n - z_m - z'') dz'' \right]$$

where

$$\begin{aligned} R_+ &= \sqrt{a^2 + (z_{nm}^+)^2}, & z_{nm}^+ &= z_n - z_m - \frac{1}{2}\Delta z \\ R_- &= \sqrt{a^2 + (z_{nm}^-)^2}, & z_{nm}^- &= z_n - z_m + \frac{1}{2}\Delta z \end{aligned} \quad (20.10.5)$$

Using the derivative $\partial_{z'} G(R) = (z - z') (1 + jkR) e^{-jkR} / R^3$, we obtain:

$$Z_{nm} = \frac{j\eta\lambda}{8\pi^2} \left[\frac{z_{nm}^+}{R_+^3} (1 + jkR_+) e^{-jkR_+} - \frac{z_{nm}^-}{R_-^3} (1 + jkR_-) e^{-jkR_-} + G_{nm} \right] \quad (20.10.6)$$

where

$$G_{nm} = k^2 \int_{-\Delta z/2}^{\Delta z/2} G(z_n - z_m - z'') dz'' \quad (20.10.7)$$

This term must be evaluated by numerical integration. With definitions (20.10.5)-(20.10.7), the discretized Pocklington equation (20.10.3) becomes:

$$\sum_{m=-M}^M Z_{nm} I_m = E_n \quad (20.10.8)$$

which can be written in the matrix form

$$Z\mathbf{I} = \mathbf{E} \quad (20.10.9)$$

with solution $\mathbf{I} = Z^{-1}\mathbf{E}$. The MATLAB function `pockling` implements this solution procedure. It has the same inputs and outputs as `hallen2` with usage:

```
[I,z,cnd] = pockling(L,a,E,Nint,type); % solve Pocklington's integral equation
```

Because the Pocklington kernel depends on R like $1/R^3$, the impedance matrix of Eq. (20.10.9) will be more singular than in the Hallén case which has a kernel that varies like $1/R$.

Specifically, for the same value of M , the condition number of Eq. (20.10.9) can be one to two orders of magnitude larger than that of Eq. (20.7.11) or (20.9.8). Moreover, the Pocklington solution requires a much higher value of M to converge to the true solution. These remarks are illustrated in the examples below.

Example 20.10.1: For antennas of length near $\lambda/2$, the sinusoidal assumption for the current distribution is approximately correct. Assuming it to be exactly sinusoidal will simplify, in Chap. 21, the treatment of parasitic arrays, such as Yagi-Uda arrays.

In this example, we calculate Hallén's and Pocklington's solutions for the currents in the three cases $l = 0.45\lambda, 0.50\lambda, 0.55\lambda$ and compare them to the sinusoidal current. The antenna radius was $a = 0.001\lambda$ in all cases. Fig. 20.10.1 shows the computed currents for the cases $M = 20$ and $M = 40$.

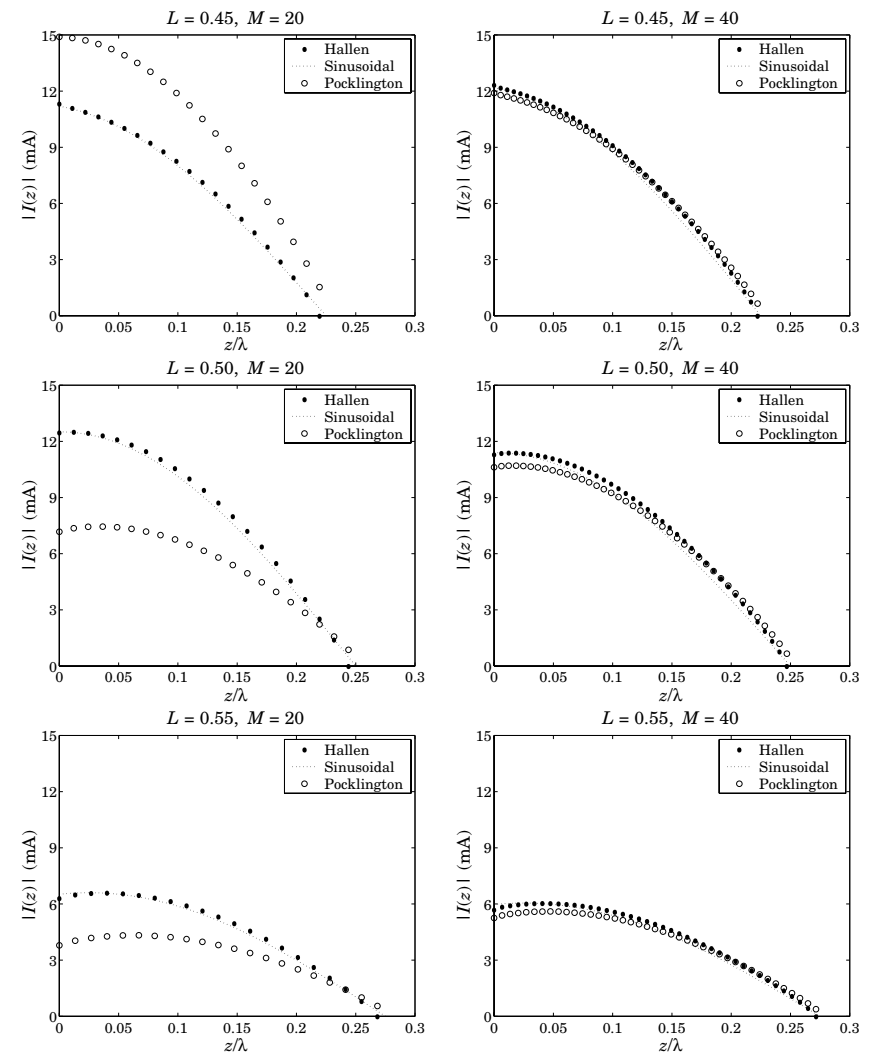


Fig. 20.10.1 Comparison of Hallén and Pocklington solutions for $l = 0.45\lambda, 0.50\lambda, 0.55\lambda$.

The Hallén solution converges for both values of M , but the Pocklington one, only for $M = 40$. Also, the condition numbers of the linear systems (20.7.11) and (20.10.9) are widely different. For example, for the half-wavelength antenna, the Hallén condition numbers are 3.24 and 5.16 for $M = 20$ and $M = 40$, but the Pocklington numbers are 943.44 and 4519.76, respectively. These graphs were produced by the following typical MATLAB code:

```
L = 0.50; h = L/2;
```

```

a = 0.001; type = 1; Nint = 16; M = 20;

Dz = h/(M+type*0.5);           spacing interval

E = zeros(2*M+1,1);  E(M+1) = 1/Dz;   delta-gap incident field

[Ih,zh,ch] = hallen(L,a,M,Nint,type);
[Ip,zp,cp] = pockling(L,a,E,Nint,type);  zp is the same as zh

Ih = abs(Ih(M+1:end));           upper half of the current
zh = zh(M+1:end);               upper half of sampled z-points
Ip = abs(Ip(M+1:end));

A = max(Ih);                     scale factor
z = 0 : Dz/20 : h;               dense set of z-points
I = kingeval(L,A,z);             sinusoidal current at z

plot(zh,Ih,'.', z,I,':', zh,Ip,'o');

```

In the above code, A is the maximum value of the Hallén current and serves as a scale factor for the sinusoidal current, that is, $I(z) = A \sin(k(h - |z|))$. The function `kingeval` simply evaluates the sinusoidal expression at a dense set of z -points. \square

Example 20.10.2: As another example, consider the cases $l = \lambda, 1.5\lambda, 2\lambda$. Fig. 20.10.2 shows the computed currents with $M = 30$ and $M = 60$.

The same slow convergence behavior of the Pocklington case is observed again. The sinusoidal current $I(z) = A \sin(k(h - |z|))$ is not a good approximation at $z = 0$ for the cases $l = \lambda$ and $l = 2\lambda$, but works well for $l = 1.5\lambda$. \square

Example 20.10.3: Next, we consider the case of a field incident at broadside ($\theta = 90^\circ$) on a linear antenna of length $l = 1.2\lambda$ and radius $a = 0.001\lambda$. Fig. 20.10.3 shows the computed currents according to Hallén and Pocklington equations, for $M = 30$ and $M = 40$.

The Hallén current was computed with the function `hallen2`. Superimposed on each graph is the current based on the sinusoidal approximation of Eq. (20.5.1), or rather, (20.5.2), that is, $I(z) = \cos kh - \cos kz$. The sinusoidal current has been normalized such that its maximum value agrees with the maximum from Hallén. Typical MATLAB code for this example was as follows:

```

L = 1.2; h = L/2; a = 0.001;
k = 2*pi; th = pi/2; M = 30;

Dz = h/(M+0.5);
zm=(-M:M)*Dz;
E = exp(j*k*zm*cos(th));

[Ih,zh,ch] = hallen2(L,a,E,16,1);
[Ip,zp,cp] = pockling(L,a,E,16,1);

z = -h:(Dz/20):h; I = cos(k*h) - cos(k*z);

Ih = abs(Ih); Ip = abs(Ip); I = abs(I); mh = max(Ih); mp = max(Ip);
I = I/max(I) * mh;
plot(zh, Ih, '.', z, I, ':', zh, Ip, 'o');

```

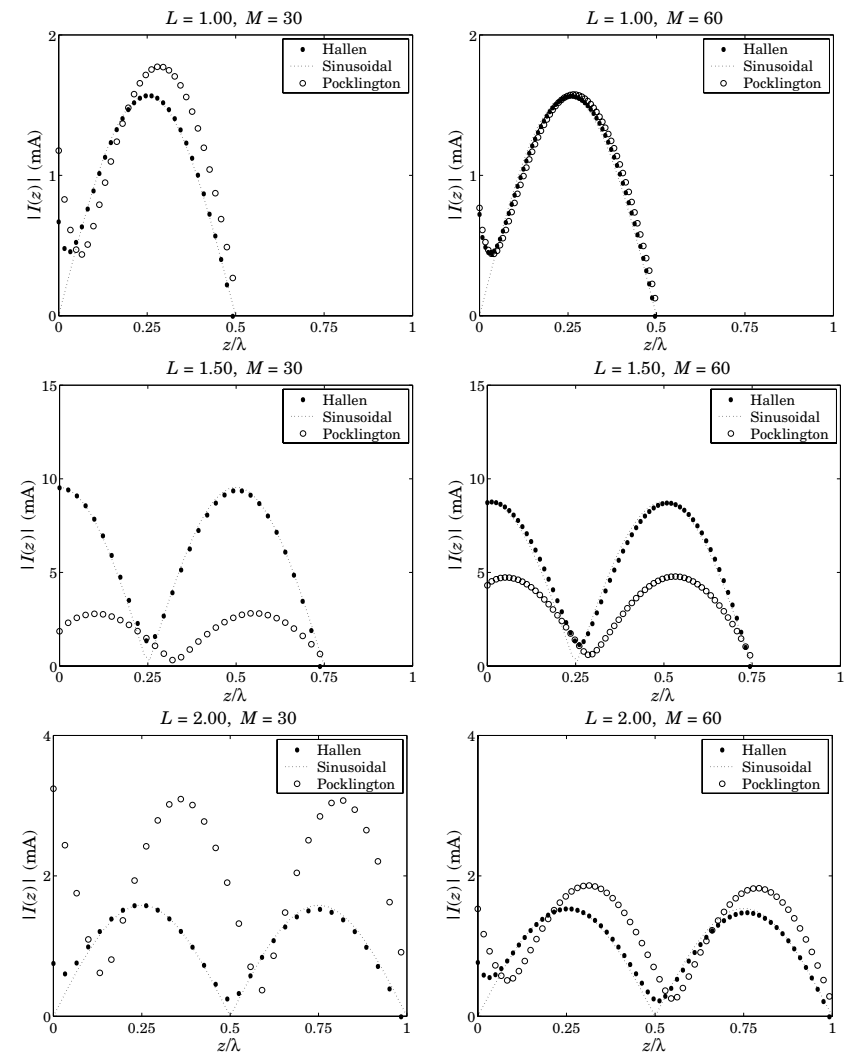


Fig. 20.10.2 Comparison of Hallén and Pocklington solutions for $l = \lambda, 1.5\lambda, 2\lambda$.

Just to emphasize the dependence of the induced current on the type of incident field, we also show in Fig. 20.10.4 the current for the delta-gap case and compare it with the sinusoidal current $I(z) = A \sin(k(h - |z|))$. In all cases, the Pocklington solution improves with increasing M . \square

We observe in all of the above examples that the Pocklington current is not required to vanish at the last sampling point, like the Hallén case. This condition was not incor-

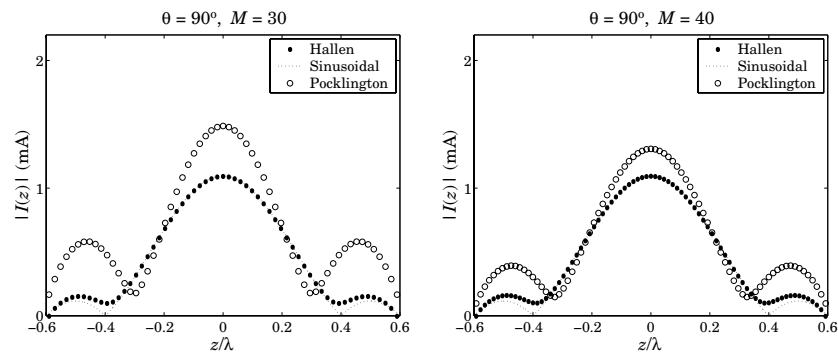


Fig. 20.10.3 Hallén and Pocklington solutions for broadside incident field.

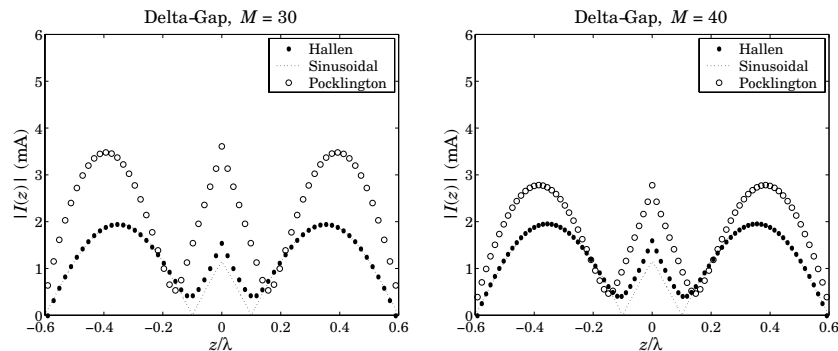


Fig. 20.10.4 Hallén and Pocklington solutions in delta-gap case.

porated into the Pocklington equation. Nevertheless, the Pocklington currents tend to zero at the antenna end-points as M becomes larger.

This entire chapter dealt with the nature of the currents on a single linear antenna. The case of several antennas forming an array and interacting with each other is treated in Chap. 21.

Hallén's and Pocklington's integral equations generalize into a system of several integral equations for the currents induced on the antennas. We solve the coupled Hallén equations in the case of delta-gap center-driven antennas. The linearity of the equations allows us to collect them together into a block matrix system from which the currents on each antenna can be obtained.

One simplification arises in the case of an array of identical antennas. Then, the block linear system can be wrapped in half much like it was done in Sec. 20.7, thus, drastically reducing the computational cost. The MATLAB function `hal1en3` implements this special case.

The case of an array of non-identical antennas is also considered and we obtain

solutions for Yagi-Uda arrays with parasitic reflector and director antennas. This case is implemented by the MATLAB function `hal1en4`.

20.11 Problems